LA-UR-19-26000
Approved for public release; distribution is unlimited.

Title: Off-Normal Scenarios Using Resistively Heated Targets

Author(s): Wass, Alexander Joseph
Woloshun, Keith Albert
Dale, Gregory E.
Dalmas, Dale Allen
Romero, Frank Patrick
Naranjo, Angela Carol
Aragonez, Robert J.
Kollarik, Nathan

Intended for: Report

Issued: 2019-06-27

Off-Normal Scenarios Using Resistively Heated Targets

Alexander Wass, Keith Woloshun, Gregory Dale, Dale Dalmas, Frank Romero, Angela Naranjo, Robert Aragonez, Nathan Kollarik

13 June 2019

Introduction

This report describes the continuation of thermal experiments using the resistively heated target assembly within the helium flow loop at LANSCE that is described in the report, Resistively Heated Target Tests Using Helium Flow Loop[1], by Alexander Wass et al. In order to replicate off-normal operating scenarios of the helium cooled Mo-100 plant design disks during beam heating, an array of resistive heaters were placed within the helium flow loop, cooled via helium, and modified slightly. The resistively heated test piece is comprised of seven ceramic electric heaters with embedded thermocouples allowing temperature measurements of each heater.

A total of three scenarios were performed. One unmodified scenario, and two off-normal scenarios were conducted to simulate a blocked cooling channel due to debris within the flow loop and a broken disk during in-beam heating at the Mo-99 production facility. A removable insert was placed within a cooling channel to block the flow of helium, and a resistive heater was removed to simulate a broken disk that had been evacuated from the target assembly. The inlet and outlet cooling pipe employs rectangular tubing to make a 90° bend at a radius consistent with and practical for the actual plant design.

Geometry

Detailed information regarding the geometry of the resistively heated target assembly and housing can be found in the previous report by Wass[1]. In these experiments, the Mo-99 plant design target disks and holder, which form rectangular helium flow channels, are replicated by rectangular heaters with embedded thermocouples available from Watlow. The heaters are mounted in a holder with 0.5 mm coolant gaps, based on past tests and analysis of target cooling with the new blower for the plant target. For the “blocked channel” and “missing disk” configurations, a stainless steel plug was inserted into the fourth cooling channel, and the third heater was removed, respectively. Figure 1 shows the heater housing and heater assembly, along with the bullnose inlet and outlet heater geometry. The heaters are inserted from the top of the housing and held in place by the heater assembly. The inlet and outlet tubing configuration contains two 90° bends at the inlet and outlet of the heater housing and is shown in Fig. 2. This tubing configuration matches more closely to the actual production plant design.

[1] A. Wass, LA-UR-18-31017, Resistively Heated Target Tests Using Helium Flow Loop, 2018

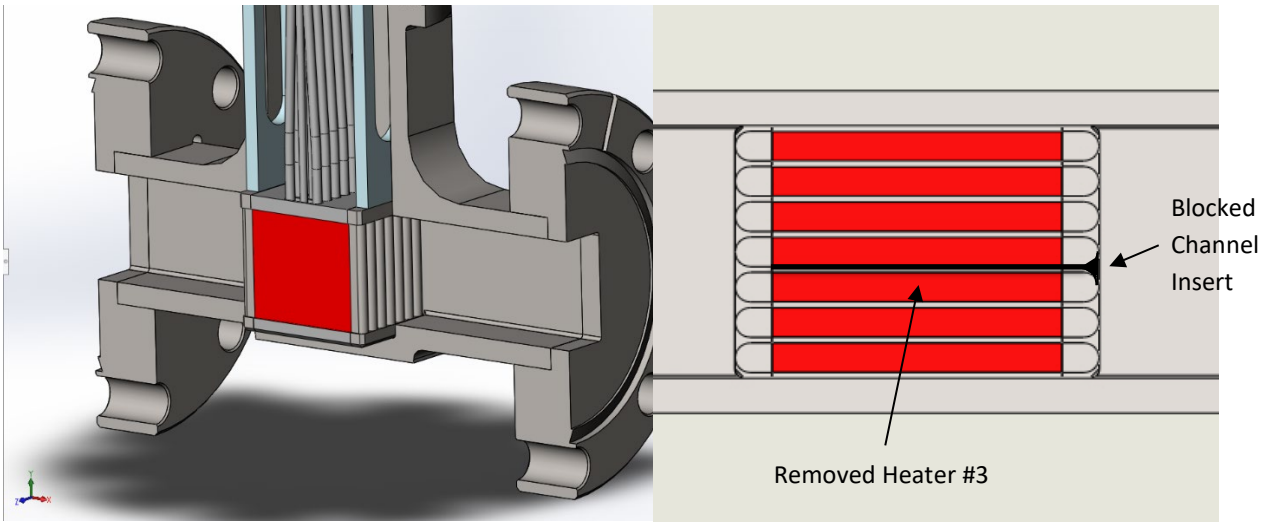

Figure 1 – Cut away view of heater housing with heaters (left) and top cross sectional view of heaters showing off-normal scenarios (right)

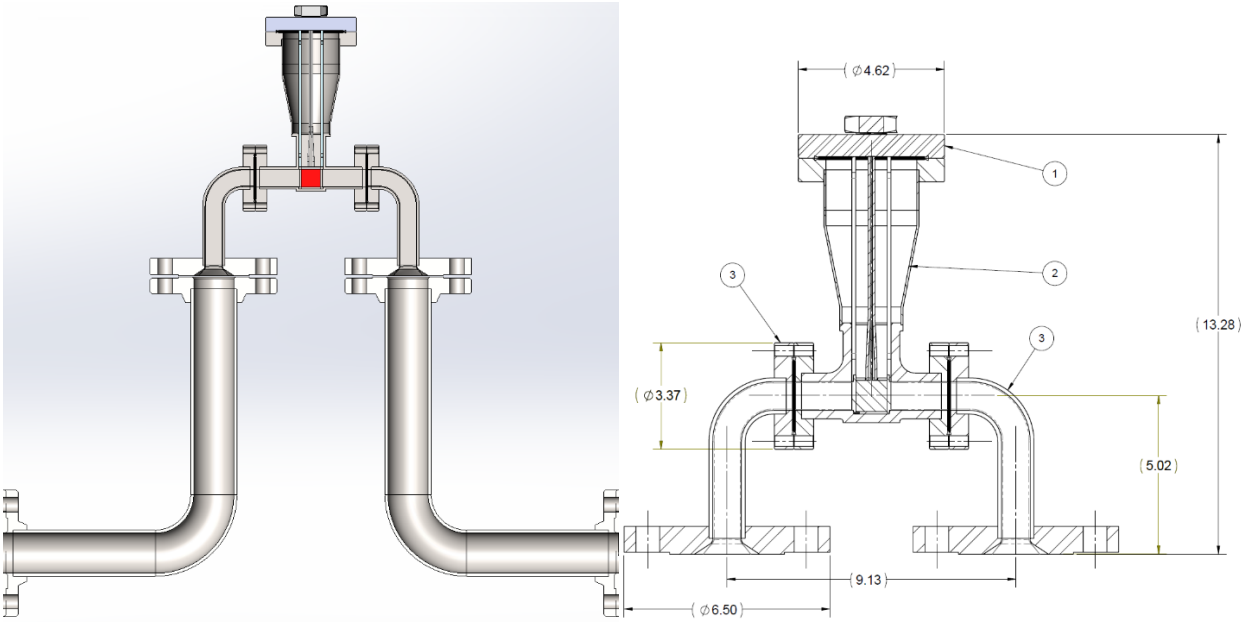

Figure 2 – 90° bent tubing configuration (left) and close-up cross section (right) similar to Mo-99 production plant design

Experiment

Setup and Instrumentation

Detailed information regarding the setup and instrumentation for these experiments can be found in the previous report by Wass[1]. For the off-normal experiments, a 0-30 psi differential pressure transducer was added across the heater housing to determine the pressure loss more accurately. The heater housing and inlet-outlet tubing configuration is shown in Fig. 3. A close-up picture of the heater inlet can be seen in Fig. 4. The helium flow rate was increased to 78 g/s (according to the turbine flow meter), and was decreased to 40 g/s in increments of ~10 g/s. The temperature of the helium and heaters were allowed to stabilize before the flow rate was changed. The heaters were maintained at

about 240-247V and up to 3.6 A per heater. Total heater power was maintained between 4860 and 5700 W depending on the off-normal scenario.

Figure 3 - Heater housing in line with the 90° bend configuration with the power breakout box in the background

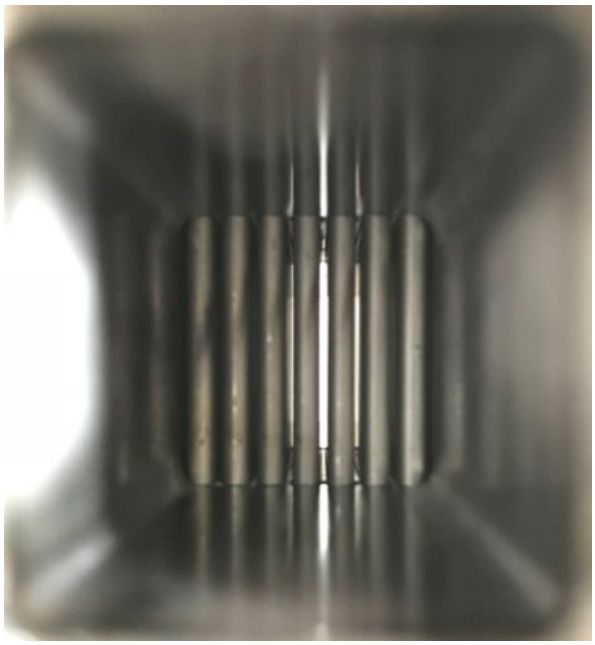

Figure 4 - Inlet view of the resistive heater array assembled in housing

Results

The inlet pressure was maintained between 315 and 330 psig with helium. Pressure drop during heating for all scenarios can be seen in Fig. 5. As expected, the pressure drop in the blocked channel scenario was much greater than both the unmodified and missing disk scenarios (25% greater) at 70 g/s. Notice that the blocked channel scenario was not performed at 78 g/s due to the pressure head limit of the blower. The unmodified and missing disk scenarios had nearly identical pressure losses. Figure 6 shows the total heater and fluid power for all three scenarios. The fluid thermal power is calculated by $q_T = \dot{m} C_p \Delta T$, where $\dot{m}$ is mass flow rate, C_p is specific heat at constant pressure, and ΔT is the temperature difference between the inlet and outlet. One can see that the fluid power is greater than the heater power by up to 4%, which is a non-realistic result. The reason behind this could be due to inaccurate flow meter data. There are two flow meters in the flow loop. One operates on a vortex principle, and the other has a small turbine that rotates due to the flow. The vortex flow meter measured consistently lower than the turbine flow meter (~8 g/s at max flow), however, the data in this report was recorded from the turbine flow meter which may slightly overestimate the mass flow rate. The actual flow rate is somewhere between the vortex and turbine flow meter outputs.

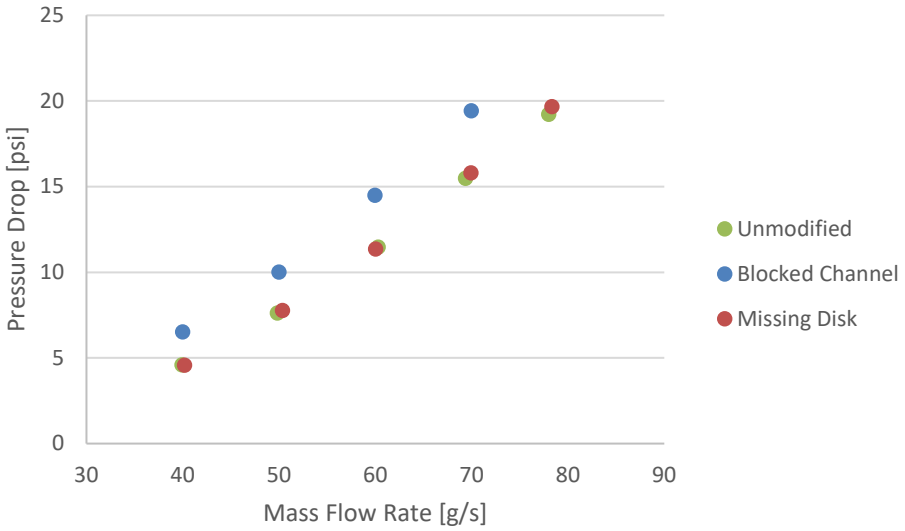

Figure 5 - Pressure drop for the unmodified, blocked channel, and missing disk scenarios during resistive heating

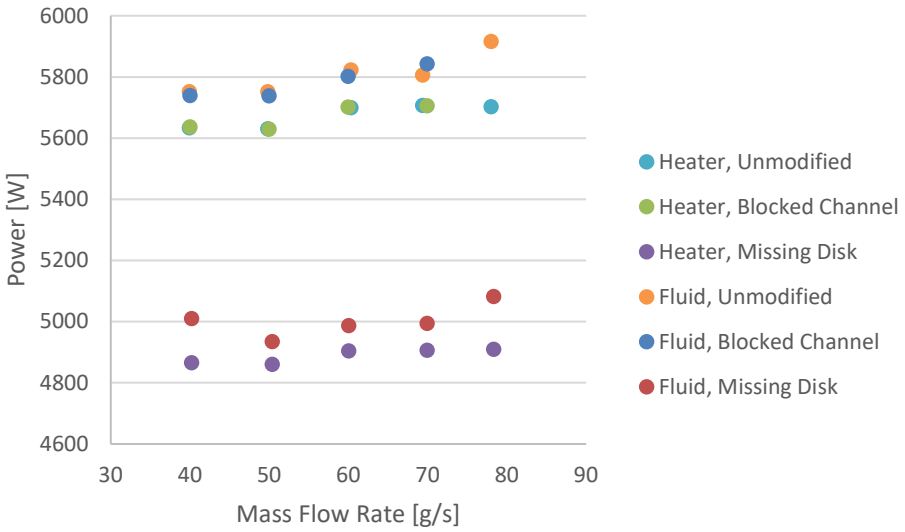

Figure 6 - Total heater power and fluid power for all scenarios

The temperature increase of the helium due to the heaters is shown in Fig. 7. The maximum temperature increase was 28°C at a flow rate of 40 g/s for the missing disk and blocked channel scenarios, and the lowest was about 12.5°C at 78 g/s for the missing disk scenario (the total heater power was 1/7th lower than the other two scenarios due to the removal of one heater). Slight variations in flow rate for the three scenarios caused slight temperature variations as well. The heater housing bottom wall temperature remained cool for all of the scenarios and flow rates and never exceeded 31°C.

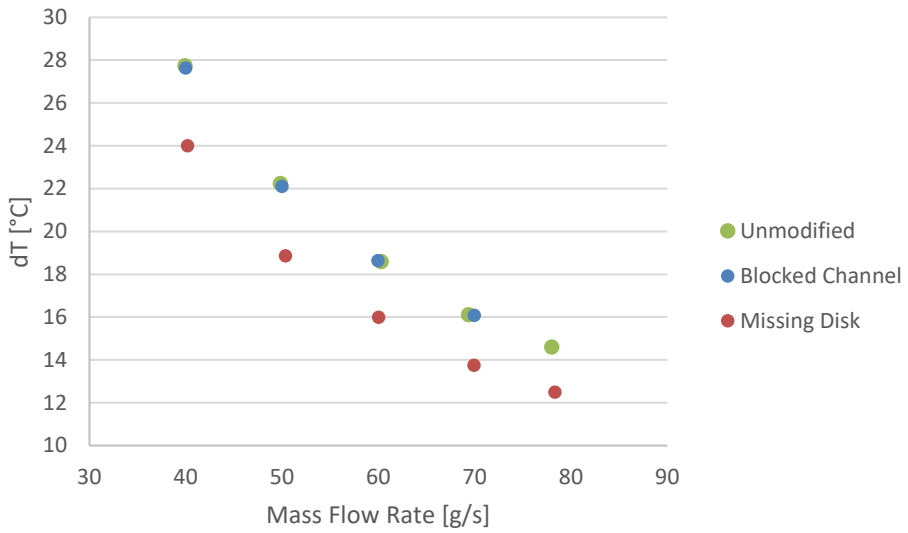

Figure 7 – Helium temperature change upstream and downstream of heaters for all scenarios

Individual heater temperatures were measured for both experiments. Since the heater electrical resistance varied randomly from 62.8 to 72.3 ohms at room temperature, shown in Fig. 8, the individual heater power varied by as much as 16%. This variation in individual heater power caused non-uniform heater temperatures. Figures 9-13 show the change in temperature between the individual heaters and the helium inlet with their respective flow rates and Reynolds numbers (unmodified scenario). For the blocked channel scenario, heaters 3 and 4 surrounding the blocked channel had temperatures up to 9.3°C greater than the unmodified scenario at 70 g/s. The temperatures for the rest of the heaters were lower by up to 3°C than the unmodified scenario due to greater flow and heat transfer in the flow channels. The missing disk scenario temperatures were consistent with the unmodified case, besides heaters 2 and 4, which were greater by up to 6.5°C at 70 g/s due to the lack of flow from the now large cooling channel.

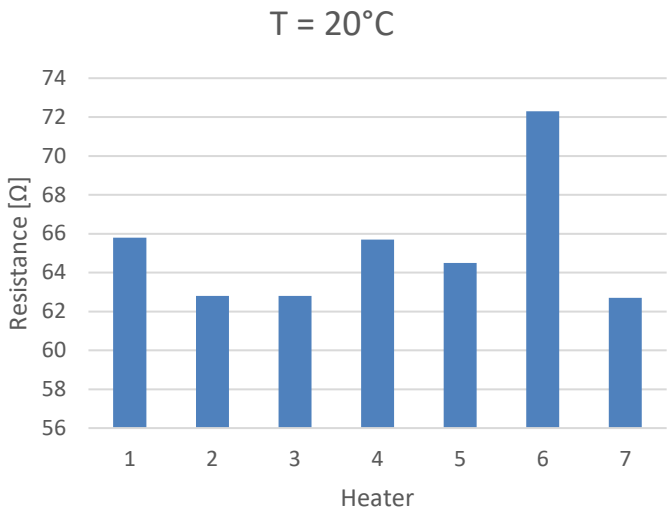

Figure 8 - Heater electrical resistance at 20°C (measured from feedthroughs)

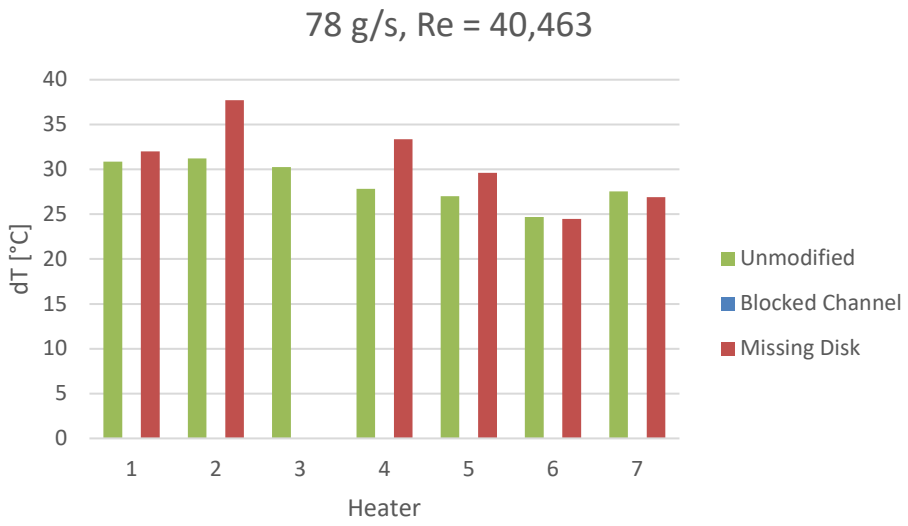

Figure 9 – Temperature change between heaters and helium inlet for two scenarios at 78 g/s

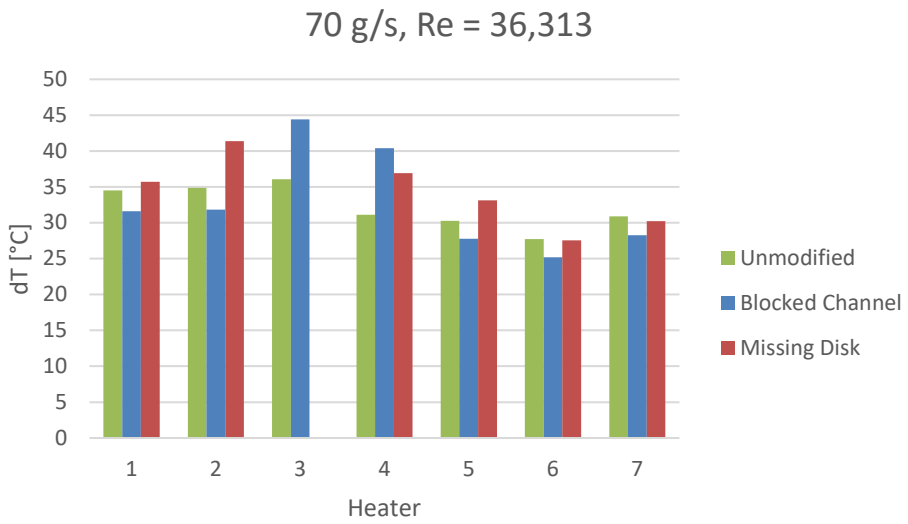

Figure 10 - Temperature change between heaters and helium inlet for all scenarios at 70 g/s

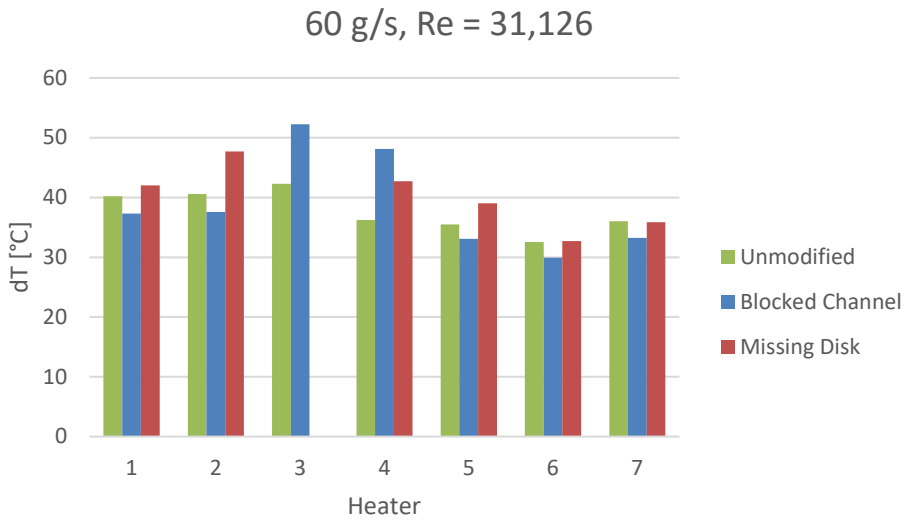

Figure 11 - Temperature change between heaters and helium inlet for all scenarios at 60 g/s

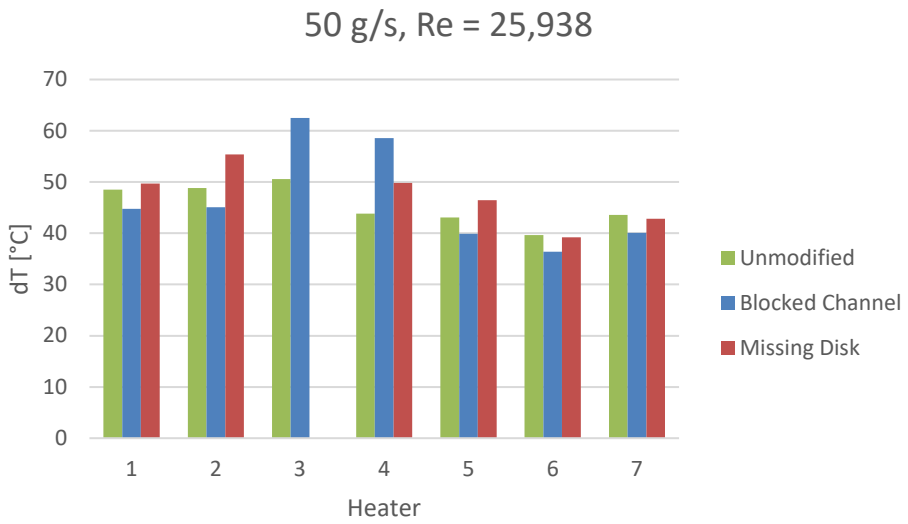

Figure 12 - Temperature change between heaters and helium inlet for all scenarios at 50 g/s

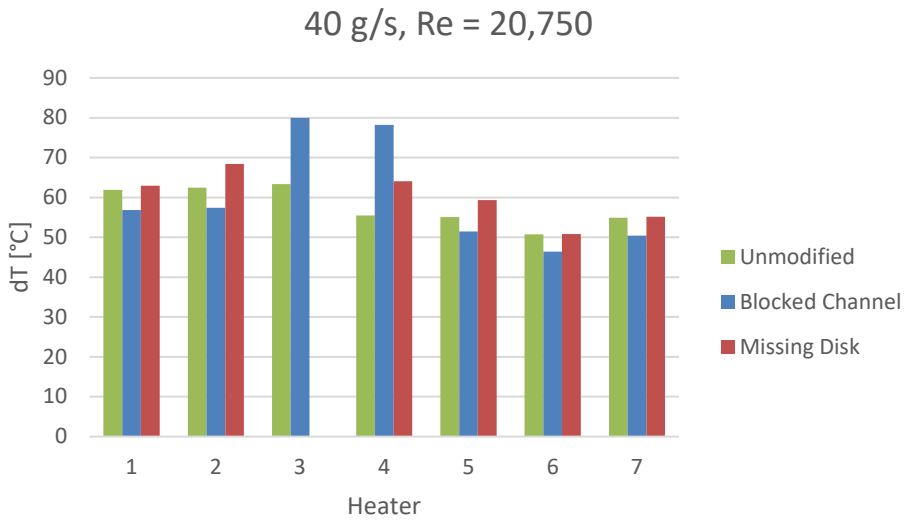

Figure 13 - Temperature change between heaters and helium inlet for all scenarios at 40 g/s

Analytical Calculations

Theory

The convection heat transfer coefficient (HTC) of the helium cooling fluid as well as other flow characteristics can be determined analytically using several fundamental fluid equations. First, the Reynolds number is used to characterize fluid flow as laminar, turbulent, or in a transition state. The Reynolds number for fluid flow in a closed channel is calculated by Eq. 1,

$$Re = \frac{\rho D_h V}{\mu} \tag{1}$$

where D is the inner pipe diameter, V is the mean fluid velocity, and μ is the dynamic viscosity of the fluid. The helium density and viscosity were determined at the mean fluid temperature according to the experiment results. The convective HTC is determined using Eq. 2,

$$h = \frac{Nu\, k}{D_h} \tag{2}$$

where k is the thermal conductivity of the fluid, D_h is the hydraulic diameter of the channel, and Nu is the Nusselt number. The Nusselt number can be expressed using the Dittus-Boelter[2] correlation for heating of a fluid:

$$Nu = 0.0243 Re^{4/5} Pr^{0.4} \tag{3}$$

[2] Incropera and DeWitt, Fundamentals of Heat and Mass Transfer, 7th Ed., Wiley, 2012, p. 544.

where $0 \leq Pr \leq 160$, $Re \geq 10{,}000$, and $\frac{L}{D} \geq 10$. The Nusselt number can also be expressed using the Gnielinski[3] correlation which is valid for smooth tubes over a larger range of Reynolds numbers and is shown in Eq. 4,

$$Nu_D = \frac{(f/8)(Re_D - 1000)Pr}{1 + 12.7(f/8)^{1/2}\left(Pr^{2/3} - 1\right)} \tag{4}$$

where $0.5 \leq Pr \leq 2000$ and $3000 \leq Re \leq 5E6$. The friction factor for smooth tubes is determined by Eq. 5.

$$f = (0.79\ln(Re) - 1.64)^{-2} \tag{5}$$

Pressure drop across the heaters with a bull nose entrance and exit was also determined analytically. The general equation for pressure change in terms of head loss can be seen in Eq. 6,

$$\Delta P = h_f \rho g \tag{6}$$

where h_f is the dynamic head for internal flow. In this experiment, the dynamic head of the flow channels in between the resistive heaters can be determined by Eq. 7,

$$h_f = \left(\frac{fL}{d_h} + \Sigma K\right)\frac{V^2}{2g} \tag{7}$$

where: ΣK is the sum of loss coefficients for the bull nose entrance and exit (0.05 and 0.5, respectively). The friction factor under turbulent conditions for various surface roughness is calculated using Eq. 8,

$$f = \left\{-1.8log\left[\frac{6.9}{Re} + \left(\frac{\frac{\varepsilon}{d}}{3.7}\right)^{1.11}\right]\right\}^{-2} \tag{8}$$

where: ε is the surface roughness of the material (m). Using these correlations, the heater wall temperature is determined by the basic convection heat transfer equation,

$$T_s = T_m + \frac{q"}{h} \tag{9}$$

where T_m is the mean fluid temperature and q" is the wall heat flux (W/m^2). Also, the surface temperature can be related to the maximum heater internal temperature, assuming that both sides are equal temperatures,

$$T_{max} = \frac{\dot{q}L^2}{2k} + T_s \tag{10}$$

where $\dot{q}$ is the internal heat generation of the heater (W/m^3), L is the length from the heater midline to the heater surface, and k is the heater thermal conductivity. In this case, the aluminum nitride heaters have a thermal conductivity of 150 W/m-K.

[3] Incropera and DeWitt, Fundamentals of Heat and Mass Transfer, 7th Ed., Wiley, 2012, p. 545.

Results

The analytical results were compared to the experimental results. First, pressure drop as a function of mass flow rate is shown in Fig. 14. The analytical results using the friction factor for smooth tubes (Eq. 5) and the general friction factor correlation (Eq. 8) for the unmodified scenario are included. One can see that the pressure drop using the general friction factor correlation matches closely with the unmodified experimental results.

The analytical and experimentally determined average heater surface temperatures are shown in Fig. 15. Since the heater temperature from the experiment was measured at the center of each heater, Eq. 10 can be used to estimate the average surface temperature. It is shown that the estimated experimental heater surface temperatures are less than the Dittus-Boelter and the Gnielinski correlations. Small variations in experimental temperatures between the three scenarios are due to inlet helium temperature fluctuations of up to 5°C. Temperature differences between the unmodified experiment and the Dittus-Boelter correlation results range from approximately 19°C at 40 g/s, to about 17°C at 78 g/s. The calculated surface temperatures from the Gnielinski equation are about 6-9°C greater than determined using the Dittus-Boelter correlation.

The average heat transfer coefficient between the heaters at various mass flow rates is shown in Fig. 16. The experimentally determined HTC values for all scenarios are determined from Eq. 9 using the estimated surface temperatures described earlier. Again, the experimental values are compared to analytical calculations. One can see how large the experimental HTC is compared to the analytical results. The unmodified experimentally determined HTC at a flow rate between 40 to 78 g/s is 65-115% greater than the Dittus-Boelter correlation, respectively. The expected HTC at 78 g/s using the Dittus-Boelter correlation is 16,405 W/m^2-K, whereas the unmodified experimentally determined HTC is about 35,274 W/m^2-K. Clearly, this is not a realistic value since this would place the HTC in the liquid water flow range. Several tests were performed and described in the previous report[1] to try to diagnose the high HTC results with no success.

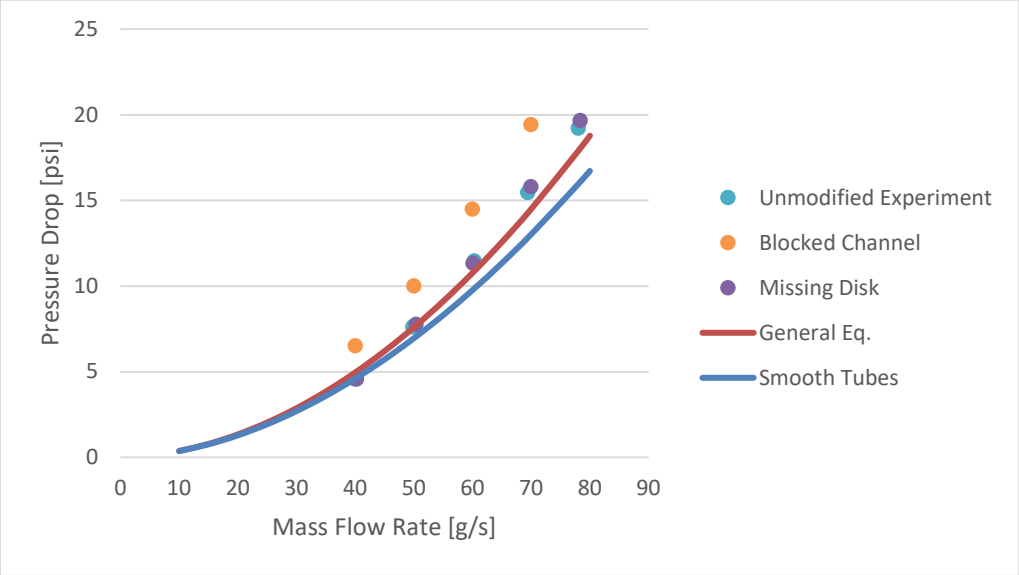

Figure 14 - Pressure drop across resistive heaters compared to theory

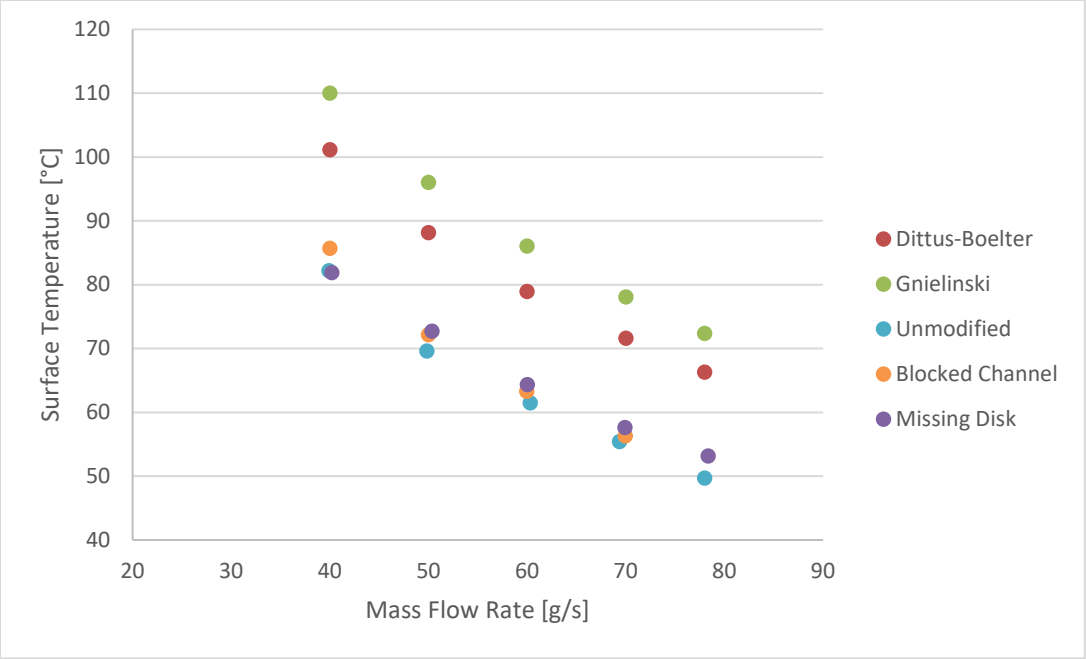

Figure 15 - Heater surface temperature comparison between theory and experimental approximations

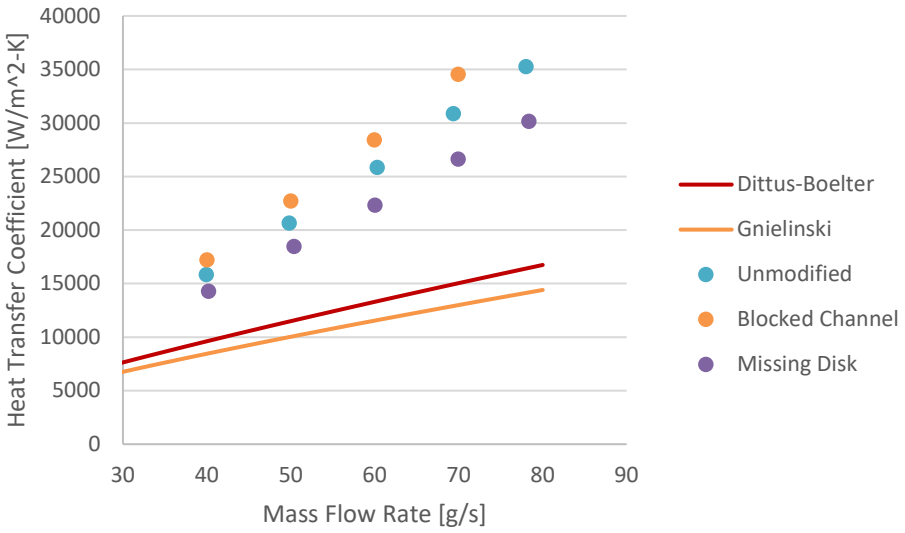

Figure 16 - Heat transfer coefficient comparison between theory and experiment

Conclusion

Three successful heater experiments were conducted for the unmodified, blocked channel, and missing disk scenarios. As expected, the blocked channel scenario restricted helium flow more than the missing disk and unmodified scenarios. The blocked channel had up to 25% greater pressure loss than the unmodified and missing disk scenarios. Pressure loss from the unmodified scenario showed good agreement with theory. For the blocked channel scenario, the heaters surrounding the blocked channel had temperatures up to 9.3°C greater than the unmodified scenario at 70 g/s. The temperatures for the rest of the heaters were lower by up to 3°C than the unmodified scenario due to greater flow and heat

transfer in the flow channels. The missing disk scenario temperatures were consistent with the unmodified case, besides the heaters adjacent to the large flow channel, which were greater by up to 6.5°C at 70 g/s.

Surface heater temperature varied widely between the experiment and theory. Up to a 28°C temperature difference at 40 g/s was seen from experiment results to theory. At 80 g/s, the results were similar. A temperature difference of 22°C from theory were determined. Additional tests need to be performed to diagnose the high temperature differences. All in all, the resistive heater off-normal scenario experiments were performed successfully, yet additional questions remain unanswered.